Cooling and Annealing Properties of Copolymer-Type Polyacetals and Its Crystallization Behavior

WEN-YEN CHIANG and MING-SONG LO, *Department of Chemical Engineering, Tatung Institute of Technology, 40 Chungshan North Road, 3rd Sec., Taipei 10451, Taiwan, Republic of China*

Synopsis

Copolymer-type polyacetals (POMs) that have been cooled at seven different rates from the melt at 180°C to the solid at 23°C show average spherulite diameters from 10 to 25 μm on an etched fracture surface using scanning electron microscopy (SEM). The wide-angle X-ray diffraction (WAXD) of POM displays a degree of crystallinity ranging from 60 to 66% by applying the two-phase model. From studies of mechanical properties, physical properties, and dielectric dissipation factor (tan δ), we found that POM with a faster cooling rate shows looser packing and smaller spherulites on the fracture surface than that with a slower cooling rate. This conclusion is in agreement with the observations made on SEM and WAXD. DSC measurements were used to measure the heat of fusion, melting point, and crystallization temperature of POMs. An equilibrium melting temperature was estimated from the Hoffman–Weeks plot. The overall crystallization kinetics of POMs were analyzed by the Avrami equation. Results for the Avrami exponent n, between 2 and 3, indicate small disklike spherulites following nucleation growth kinetics. Annealing the cooled POM at 150°C results in recrystallization featuring a significant increase in the average diameter of spherulites in SEM.

INTRODUCTION

As outlined in previous papers,[1-5] much effort has been devoted to the effect of molecular weight on fatigue crack propagation in polyacetal resins. As reviewed by Fitchmun and Newman,[6] the crystalline structures obtained depend on cooling rates, mechanical stress, mold surface, and other factors. Either spherulitic or transcrystalline surface morphology is obtained on polypropylene depending on the cooling rate. Maxwell and co-workers[7] reported the effects of shear stress on the crystallization of linear polyethylene and poly(1-butene). The effect of annealing a semi-crystalline polymer[8,9] changes in molecular mobility, morphology, and physical property.

In our report, the purpose in studying the morphology of semicrystalline polymers is to be able to understand the properties and thermal behavior of copolymer-type polyacetals. First, we report on the mechanical and physical property changes of copolymer-type polyacetal (POM) related to the effects of the mold-cooling condition in the temperature range from the region of fusion at 180°C to that of the solid at 23°C. Second, differential scanning calorimeter (DSC) was used to discriminate the copolymer-type polyacetals on the basis of their heat of fusion (H_f), melting temperature (T_m), and crystallization temperature (T_c). Isothermal studies were used to investigate the kinetics of crystallization.

Journal of Applied Polymer Science, Vol. 34, 1997–2023 (1987)
© 1987 John Wiley & Sons, Inc. CCC 0021-8995/87/051997-27$04.00

EXPERIMENTAL

Materials

Two commercial copolymer-type polyacetals, Duracon M90 (POM-I) and Duracon M270 (POM-II) with melt flow indexes of 9.0 and 30.5, were used. Both polymers have the $-CH_2O-$ group as a repeating unit. Their thermal stability increases with ethylene oxide content. The etching solution is a chromic acid mixture, which is prepared from potassium dichromate, concentrated sulfuric acid, and distilled water at the ratio of 4:100:8 by weight.

Cooling, Annealing, and Etching Processes

The compression molding of copolymer-type polyacetals (POMs) into a sheet of 2.5–3.0 mm thickness was done at 150 kg/cm^2 at 180°C and cooled at: 5, 10, 30, 45, 60, 75, and 350°C/min, from the melt at 180°C to the solid at 23°C. In the annealing process, the cooled POM samples were annealed at 150°C under forced-air ventilation. All the samples that fractured in liquid nitrogen were etched by mixed chromic acid for 25 s at room temperature, washed with distilled water, and dried at 65°C in the oven for 30 min.

X-Ray Measurements

The X-ray diffraction profile was measured on a Rigaku vertical goniometer using FeKα radiation generated at 50 kV and 50 mA. A teletype was connected to the terminal of the digital counter so that the number of counts was automatically recorded. Intensities were counted at 0.05–1.0° intervals in the Bragg angle (2θ). The degree of crystallinity (X_c) was calculated from the diffraction peak by determining the ratio of the crystalline area to the total area. Thus, the X-ray diffraction from a two-phase model is assumed to be additive. The diffracted intensity is

$$X_c(\%) = (I_c/I) \times 100\%$$

where X_c is the degree of crystallinity, I_c is the intensity area between $2\theta = 27$ and 30°, and I is the intensity of the total area from $2\theta = 19$–35°. The perfect crystals give narrow diffraction peaks, whereas semicrystalline polymers show broad diffraction peaks. This broadness is interpreted as resulting from the small size and the imperfection of the polymer crystals.

Mechanical Measurements

Tensile properties were measured by the ASTM D638 test method with the Instron Universal Testing Machine Model 1130. The crosshead load was at 500 kg, speed 5 cm/min, and chart speed 100 cm/min. Notched Izod impact strength was measured by the ASTM D256 test method by using Charpy type of a thickness of about 0.4 ± 0.02 cm and the energy was at 60 kg cm. Mold shrinkage was measured by the ASTM D995 test method.

Density Measurements

The density was measured at 23°C and was used to calculate the specific gravity of the plastics by displacement (ASTM D792). The calculation was

based on the following:

$$\text{sp gr } 23/23°\text{C} = a/(a + w - b)$$

where a is the apparent weight of the specimen without a wire or sinker in air, b is the apparent weight of the specimen (and of the sinker) completely immersed and of the wire partially immersed in pure water, and w is the apparent we[illegible] f the totally immersed sinker and of the partially immersed wire. Thus, [illegible]ensity of POM was calculated from

$$D\,(\text{g/cc}) = \text{sp gr } 23/23°\text{C} \times 0.9975$$

Dielectric Dissipation Factor Measurements

The dielectric dissipation factor ($\tan\delta$) of the POM samples, which were molded into sheet specimens of 1.5 mm thickness, were measured by the capacitance and arc loss at a frequency of 1 MHz (ASTM D150):

$$\tan\delta = K''/K'$$

where K'' is the loss index and K' is the relative permittivity.

Thermal Analysis

A DuPont 951 differential scanning calorimeter was used to study thermal history. About 16 mg of each sample was melted at 200°C for at least 5 min and then cooled to 30°C to allow the polymer to crystallize under the same thermal condition. At this point the sample was reheated at 5°C/min to 200°C, at which temperature the sample remained for 1 min before it was rapidly cooled to the crystallization temperature (T_c). The melting point was observed to occur at about 161.0–161.6°C. The crystallization exotherm is a function of time as obtained from the isothermal crystallization experiments from which the kinetics of the crystallization was estimated. The melting enthalpy (H_f) was calculated by integrating the area under the melting endotherm of the DSC trace using the equation

$$H_f = (A \times B \times E \times S)/M$$

where A is the peak area (cm^2) under the curve, B is the time base (min/cm), E is the cell calibration coefficient, S is the sensitivity (J/min cm), and H_f is the sample's heat of fusion (J/g). Also, the 100% crystalline heat of fusion (H_f^0) of the POM was calculated by the following equation:

$$H_f^0 = H_f/X_c$$

where X_c is the degree of crystallinity calculated from the diffraction peak by finding out the ratio of the crystalline area to the total area.

SEM Photographs

Scanning electron photomicrographs (SEM) of the fracture surface of unetched and etched samples with gold of 150 Å thickness were taken on a Cambridge Stereoscan Mark II 150.

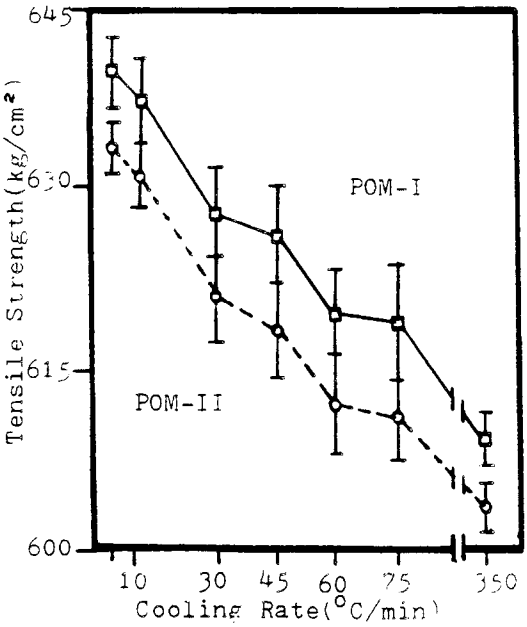

Fig. 1. Tensile strength of copolymer-type polyacetals at different cooling rates.

RESULTS AND DISCUSSION

Since we are concerned with correlating the small scale crystalline structure with mechanical and physical properties, and dielectric dissipation factor of copolymer-type polyacetals, it is important to determine whether or not cooling conditions are a deciding factor. Also bulk crystallization measurements of the POM were studied to estimate the kinetics of crystallization.

Mechanical Properties

The stress–strain properties of POM depend on different cooling conditions, that is, tensile strength, Young's modulus, elongation, and impact strength vary with the cooling rate. These effects are illustrated in Figures 1–4. As the POM cools down from the melting point, its degree of crystallinity increases with the cooling rate while the impact strength decreases, as shown in Figures 5 and 6. This effect would tend to increase tensile strength (Fig. 1) and Young's modulus (Fig. 2) but decrease elongation (Fig. 3) and impact strength (Fig. 4) because larger spherulites make POM material more brittle. The brittleness may result from the strains imposed on the amorphous phase by the crystals or from a reduction in the amount of free volume.[10,11] In general, increasing the molecular weight tends to increase toughness and the number of tie molecules. Consequently, higher molecular weight polymers tend to be more ductile and to have higher tensile strength. Also, crystallinity of the POMs of the same grade modifies the stress–strain curve by at least two mechanisms. First, the crystallites act as crosslinks by tying segments of many molecules together. Second, having very high modulus compared to the amorphous parts, the crystallites behave as rigid fillers in an amorphous

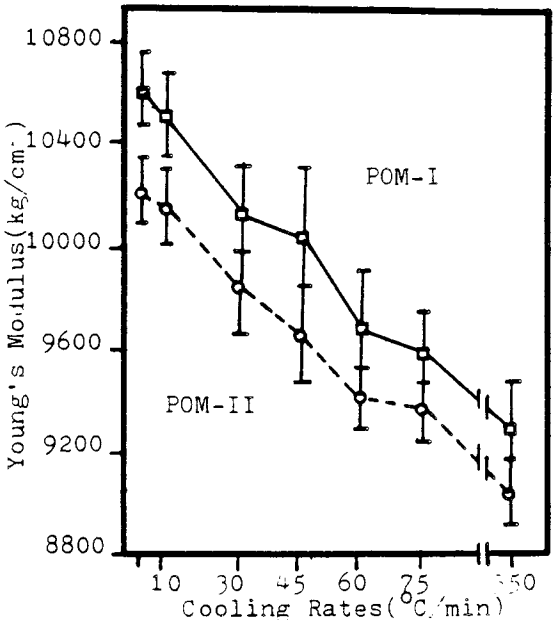

Fig. 2. Young's modulus of copolymer-type polyacetals at different cooling rates.

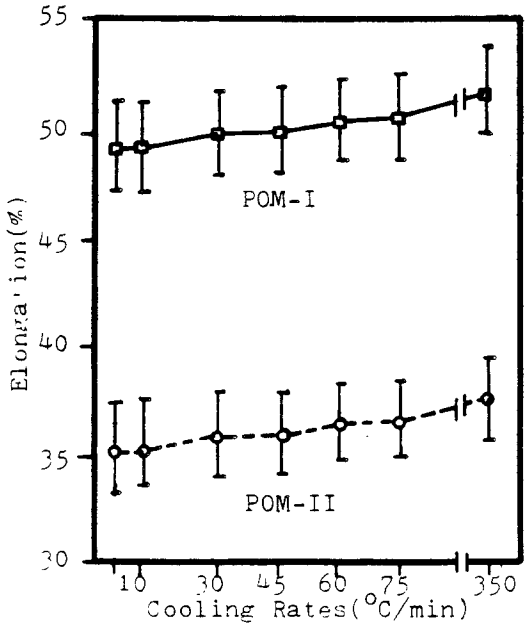

Fig. 3. Elongation at break of copolymer-type polyacetals at different cooling rates.

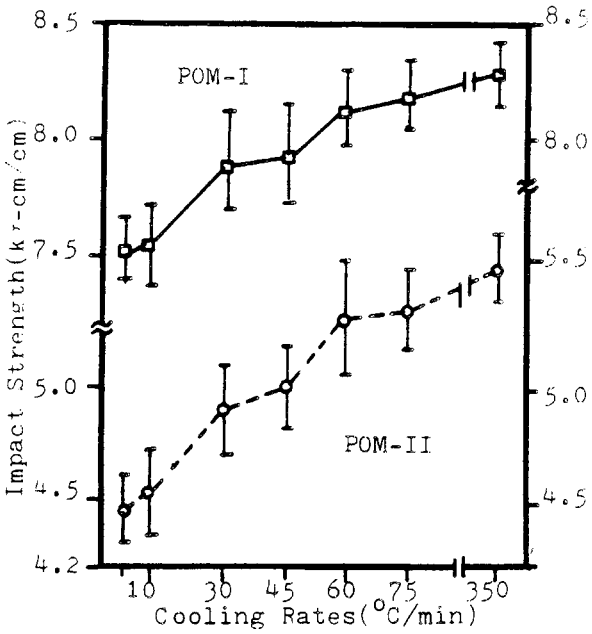

Fig. 4. Izod impact strength of copolymer-type polyacetals at different cooling rates.

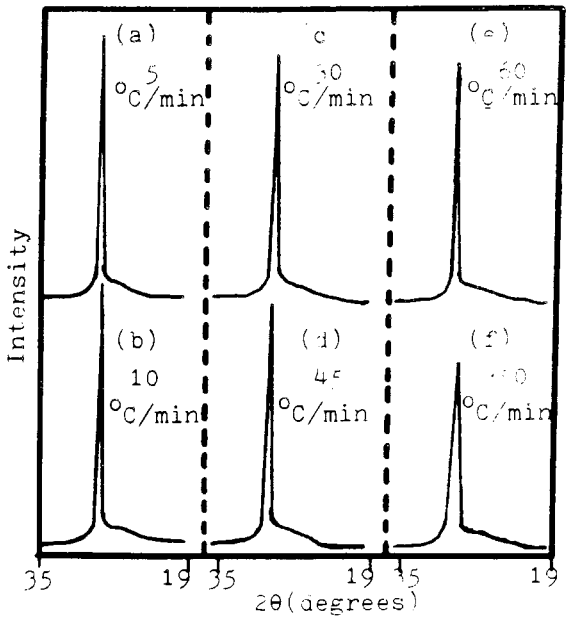

Fig. 5. Wide-angle X-ray diffractometer scans of cooled copolymer-type polyacetal (POM-I).

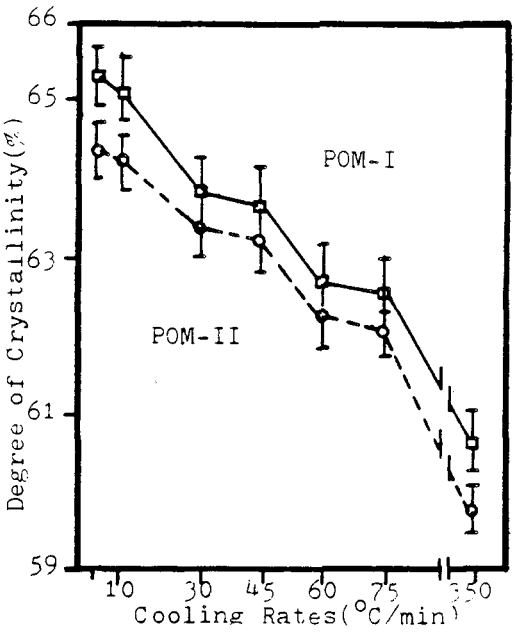

Fig. 6. Degree of crystallinity of copolymer-type polyacetals at different cooling rates.

matrix. Thus, the tensile strength and modulus increase with the degree of crystallinity among POMs of the same grade.

Physical Properties

The degree of crystallinity was calculated on the assumption that semicrystalline copolymer-type polyacetal is a two-phase model. The higher crystallinity of the POM results in an increase in the mold shrinkage, as shown in Figure 7. The crystallinity of POMs increases on account of the slow cooling from the melting point. This effect tends to reduce the amount of free volume but increases the density of packing (Fig. 7). The density of the amorphous phase will be smaller than that of the crystalline phase.

The Dielectric Dissipation Factor

A higher crystallinity should result in a lower dielectric dissipation factor, as shown in Figure 8, because of denser packing between the lamellae and larger spherulitic structures. Thus both Young's modulus and the dielectric dissipation factor are a function of mobility. A slowly cooled POM shows higher density and denser packing than a quickly cooled one.

Thermal Analysis

Melting Behavior. The melting point (T_m), crystallization temperature (T_c), heat of fusion (H_f), degree of crystallinity (X_c), and density obtained for two POMs are listed in Table I. Figure 9 shows the equilibrium melting point

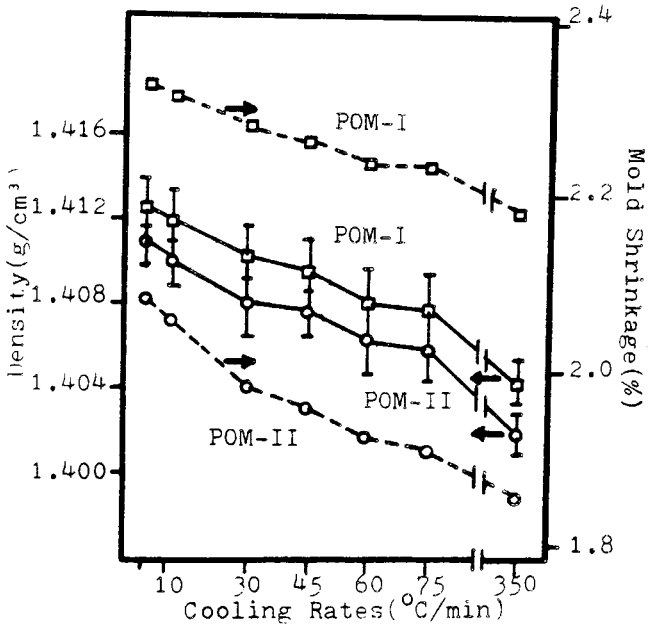

Fig. 7. Density and mold shrinkage of copolymer-type polyacetals at different cooling rates.

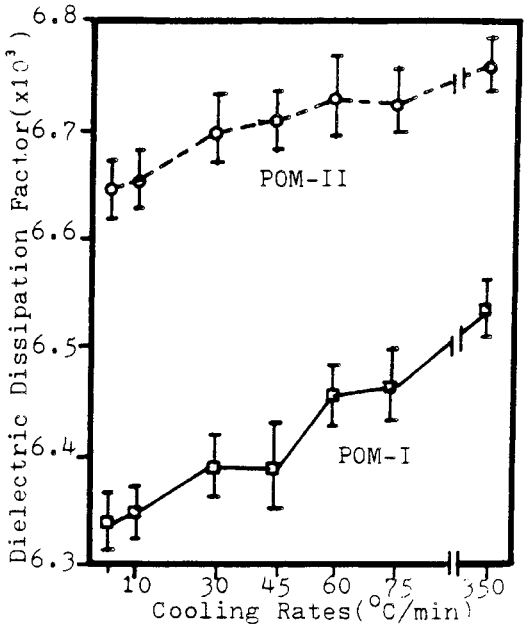

Fig. 8. Dielectric dissipation factor of copolymer-type polyacetals at different cooling rates.

TABLE I
Heat of Fusion (H_f), Degree of Crystallinity (X_c), Melting Point (T_m), Crystallization Temperature (T_c), and Density for POM-I And POM-II

Sample	H_f (J/g)	$X_c \times 100\%$	Density (g/cc)	T_m/T_c (°C)
POM-I	162.8	63.2	1.410	161.6/146.6
POM-II	161.0	62.6	1.408	161.0/145.9

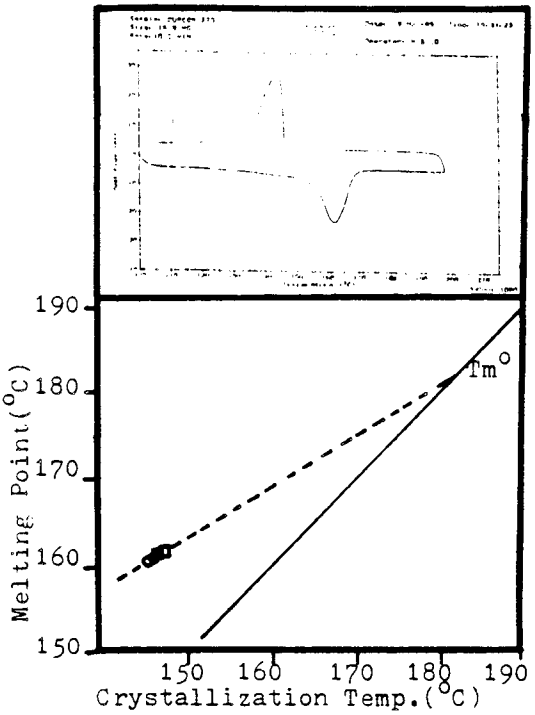

Fig. 9. An estimate of the equilibrium melting point from the Hoffman–Weeks plot yield 182.6°C [the trace of the copolymer-type polyacetal (POM-I) specimen at a heating or cooling rate of 5°C/min].

(T_m^0) at about 182.6°C using the method suggested by Hoffman and Weeks[12]:

$$T_m^0 = T_c$$

A theoretical value for the 100% crystalline heat of fusion of the copolymer-type polyacetal (H_f^0) was measured by using

$$H_f^0 = H_f/X_c$$

where H_f and X_c values were obtained from Table I. H_f^0 was calculated to be about 257.4 J/g.[13] Generally, the melting point of a crystalline polymer can be expressed as

$$\left[(1/T_m) - (1/T_m^0)\right] = \left[(-R/H_f) \times (\ln X_a)\right]$$

where H_f is the heat of fusion per mole of the repeating structural units of the polymer chain, R is the gas constant, and X_a is the mole fraction of a units in the copolymer consisting of a few of the ethylene oxide units randomly copolymerized with a preponderance of a units.

Kinetics of Crystallization. The transformation of a supercooled polymer melt into a solid crystalline phase involves two distinct steps: the birth of crystallites, termed primary nucleation, and the propagation of the individual crystallites, called growth. Primary nucleation can occur either heterogeneously or homogeneously. Homogeneous nucleation occurs via thermal fluctuations in the melt, which results in the continual formation and disappearance of crystalline clusters of molecules. Homogeneous nucleation occurs more rapidly at high degrees of supercooling. In heterogeneous nucleation adventitious impurities, residual crystalline polymer is not completely melted, or the container wall may serve as a nucleating agent. The bulk crystallization rate of selected POMs is given by the Avrami equation, and a double-logarithmic form of Avrami equation[14,15] is used to evaluate crystallization data:

$$X_t = X_0 \times [1 - \exp(-K \times t^n)] = H_t/H_0$$

$$\ln[-\ln[1 - (X_t/X_0)]] = \ln K + (n \times \ln t)$$

where X_t is the degree of crystallinity at time t, X_0 is the equilibrium crystallinity, H_t is the enthalpy of crystallization at time t, H_0 is the enthalpy of the completed transformation, and K and n are parameters related to the growth and nucleation mechanisms of the sample. The intercept gives the rate constant in the Avrami equation, which can alternatively be calculated from the simple relation:

$$1/t' = [(n - 1) \times K]/n$$

where t' is the time, at which (X_t/X_0) equals 0.5. Experimentally, from

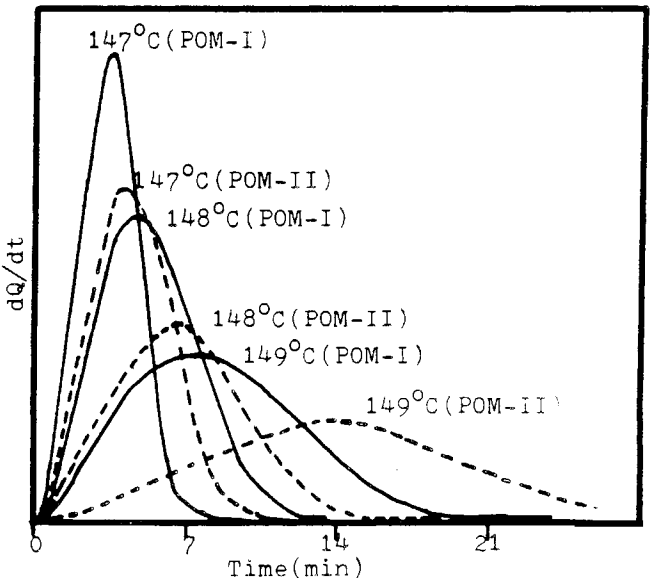

Fig. 10. Isothermal DSC traces of copolymer-type polyacetals crystallizing at different temperatures.

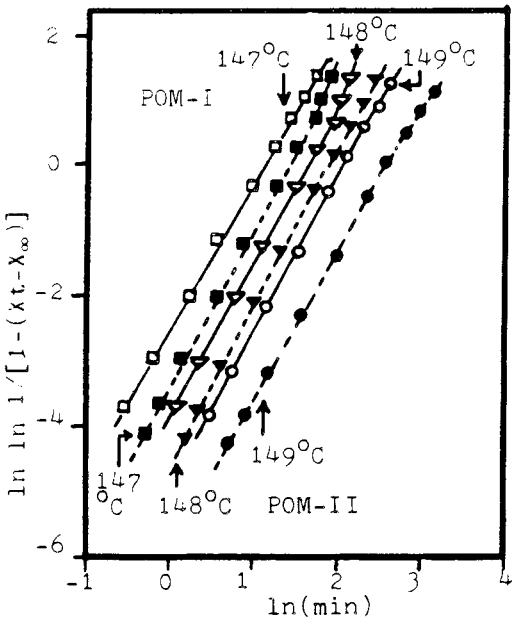

Fig. 11. Avrami double-log plots of untransformed mass fraction of copolymer-type polyacetals with log time obtained from Figure 10.

Figures 10 and 11, noninterger values of n were obtained for random heterogeneous or homogeneous nucleation and a partial crystal morphology as observed by using SEM. However, the Avrami equation depends upon a large number of assumptions: constants rate of radical growth; uniqueness of the nucleation mode; complete crystallinity; constant value of radical density; no secondary nucleation; and absence of overlap between the growing crystallization front.[16-18] Towards the end of the transformation, growing crystals deplete the supply of amorphous melt and impinge[19] upon each other. The inability to accurately discriminate between primary and secondary crystallization phenomena results in noninteger values of n. Table II shows that the noninteger values of n to be between 2 and 3, indicating that spherulites are small disklike. The kinetics indicate that not all of the crystallization occurs at the growing spherulite interface (primary crystallization), but some may occur at a later time within the spherulite already formed. The secondary crystallization involves the formation of crystals between the already formed lamellae, which may come from less crystallizable material rejected during

TABLE II
Avrami Coefficients of POM-I and POM-II

Sample	T_x (°C)	ln K	n	t' (min)
POM-I	147	−2.6	2.28	3.2
	148	−3.8	2.15	4.1
	149	−4.7	2.16	7.2
POM-II	147	−3.7	2.57	4.6
	148	−4.5	2.35	6.2
	149	−5.7	2.25	14.0

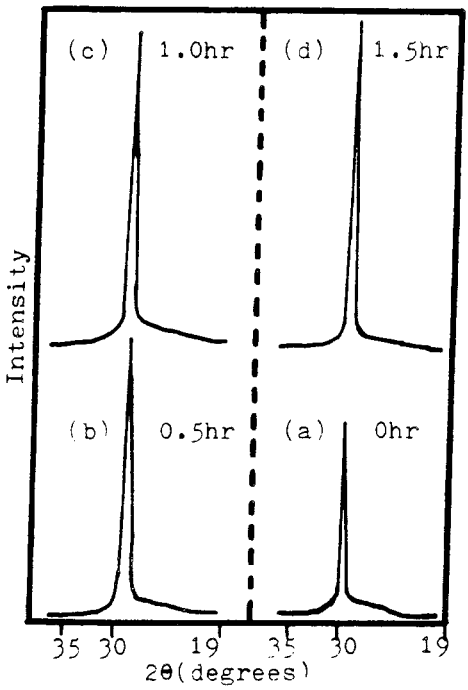

Fig. 12. Wide-angle X-ray diffractometer scans of the cooled copolymer-type polyacetals (POM-I) at 75°C/min annealing at 150°C for different times.

primary crystallization. Figures 10 and 11 are sets of isothermal DSCs traced from POM-I and -II at three different temperatures as a function of time. The rate of crystallization increases with the decrease of temperature, a characteristic of nucleation controlled growth. Also there is a significant difference between the area under the crystallization exotherms and the melting endotherms (Fig. 9). This means that further organization and crystallization must occur after the process observed in the DSC isotherms is complete.

Annealing Analysis

One of the early observations made on polymer crystals was that the thickness of the lamellae increased on annealing above the crystallization temperature but below the melting point.[20] Since the chains are folded within the lamellae, this lamellae thickening means an increase in the crystal size. A mechanism for this was suggested by Reneker.[21] He proposed that a point defect could move along the chain and result in a snakelike motion, which would in turn result in a larger crystal size being stable at a higher temperature. From the two-phase model of POMs, the X-ray diffraction from the amorphous material is determined by drawing a smooth curve through the minimum of the diffraction. The curves as shown in Figures 12 and 13 are from specimens annealed at 150°C but in four different times: 10 min, and 0.5, 1, and 1.5 h. The crystallinity keeps on increasing steadily in the first hour during annealing. At the same temperature, the degree of crystallinity as a function of annealing time of the POM shows that the degree of crystallinity rises from 63.8 to 70% in 1.5 h. Similarly, annealing the cooled specimen leads

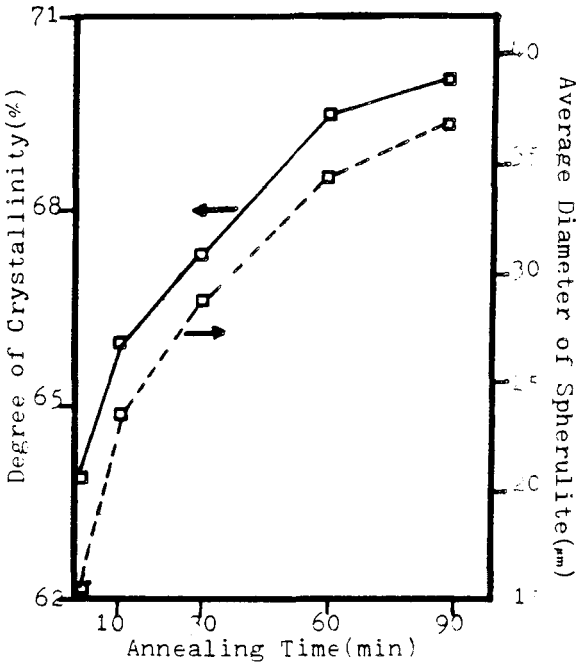

Fig. 13. Degree of crystallinity and average diameter of spherulite as a function of annealing time at 150°C of copolymer-type polyacetal (POM-I).

both to an apparent change in the average diameter of the spherulite and to the thickening of the lamellae.

Unetched and Etched Morphologies

A characteristic feature of bulk-crystallized polymers is the occurrence of spherulite morphology. Such spherulites are an aggregation of crystals and, as a consequence, an increase in the sporadic growth of crystals from heterogeneous nuclei. When a melt polymer cools and solidifies, an amorphous surface is usually formed, although its bulk phase is semicrystalline. Fractions that are not accommodated in the crystalline structure are ejected to the surface. Crystalline polymer surfaces may be transcrystalline, spherulite, or lamellae, depending on the cooling rate and nuclei activity of the mold surface. When nuclei are formed only sporadically on the surface, a spherulitic morphology can be obtained.

The SEM results of unetched and etched fracture surface morphology of seven different cooled POMs are shown in Figure 14. The unetched fracture surface morphologies of POMs indicated in Figure 15 show stress whitening and a rough fracture surface. Microphotographs in SEM display crisp and facetlike markings over the fracture surface. Direct microscopic observations indicate that the deformation is localized at the spherulite centers and at the intersection of boundaries, in agreement with mechanical properties.[22] From pictures of the unetched fracture surface, one can observe that the dimension of facetlike markings are from 20 to 50 μm. The fracture surface morphology of a slowly cooled POM is rougher than that of a quickly cooled one. The acid-etching procedure preferentially removes amorphous regions. With the

(A.1) X 2500

(A.2) X 1000

Fig. 14. SEM photomicrographs of a cross section of the internal structure of copolymer-type polyacetal: (A.1) not acid-etched; (A.2) acid-etched; (B.1) larger facetlike markings, suggesting the aggregation of two spherulites (unetched); (B.2) larger facetlike markings suggesting the aggregation of two spherulites (etched).

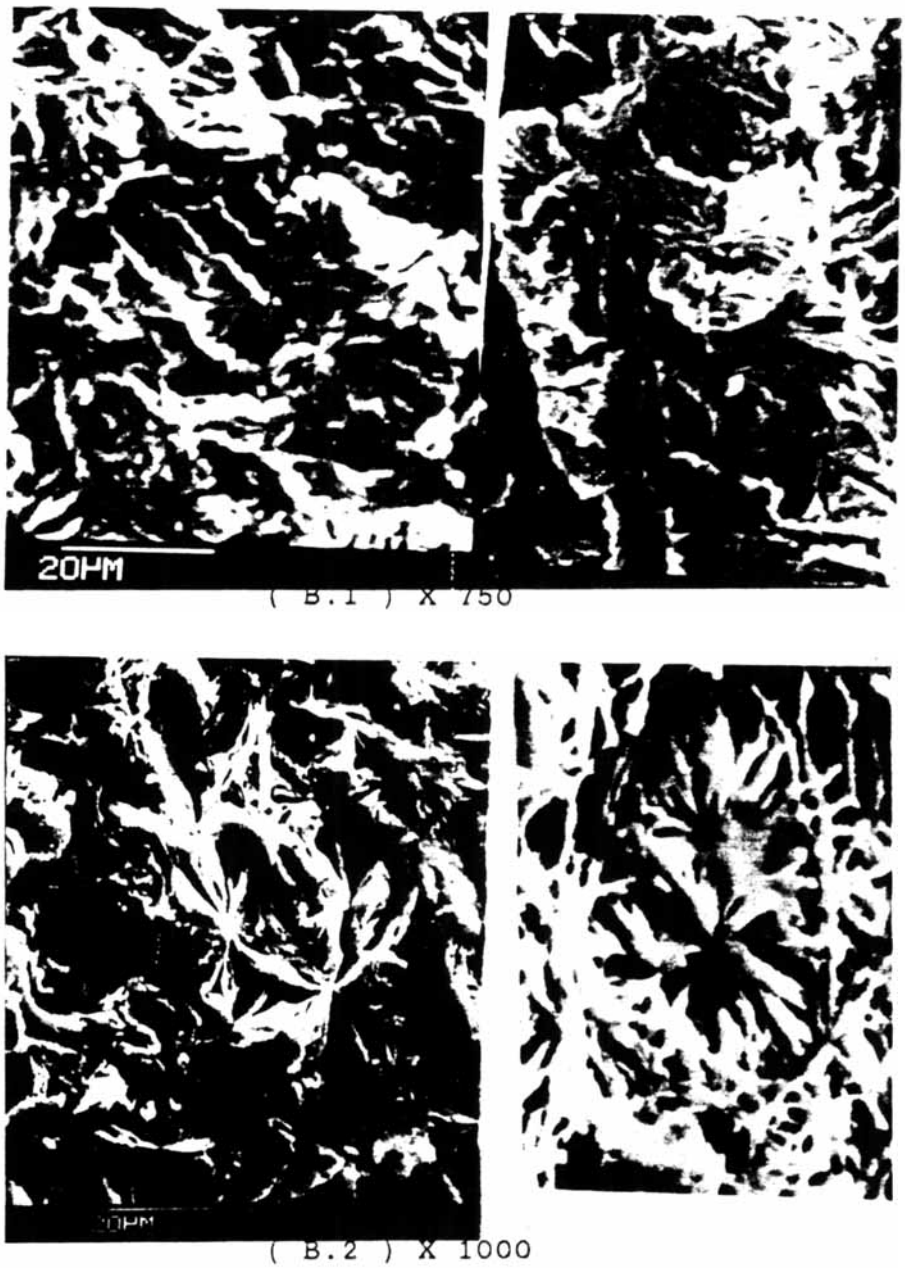

Fig. 14. (*Continued from the previous page.*)

removal of these amorphous regions, the highly complex cavities on the etched surface show up. As a result, the original crystalline morphology emerges now that the cavities are clearly visible. In case of copolymer-type polyacetals, the sample's crystalline morphology will decide the fracture surface after acid etching is done. However, it is the cooling rate of the mold that affects the crystalline morphology under investigation. At slower cooling rates, POMs can

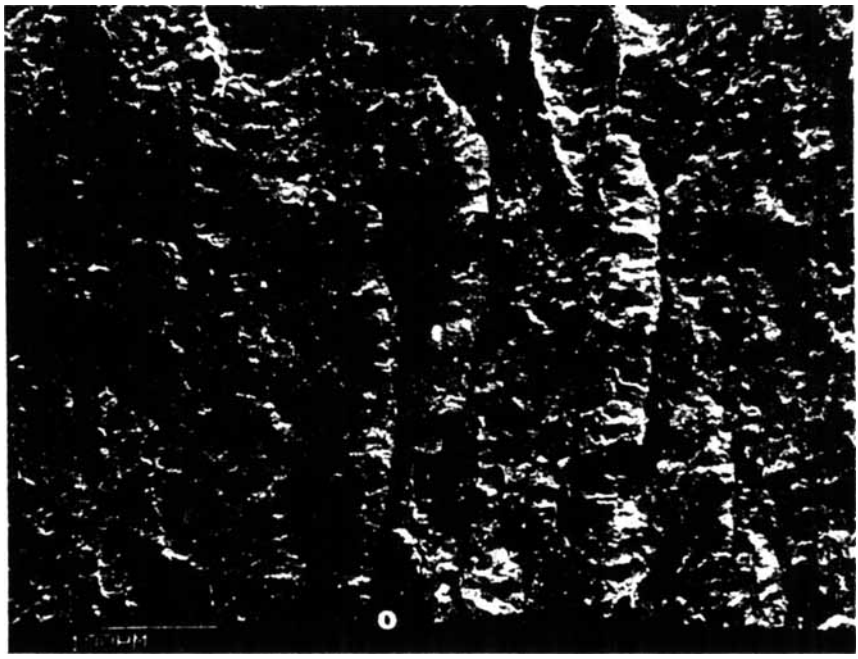

(A.1) X 150

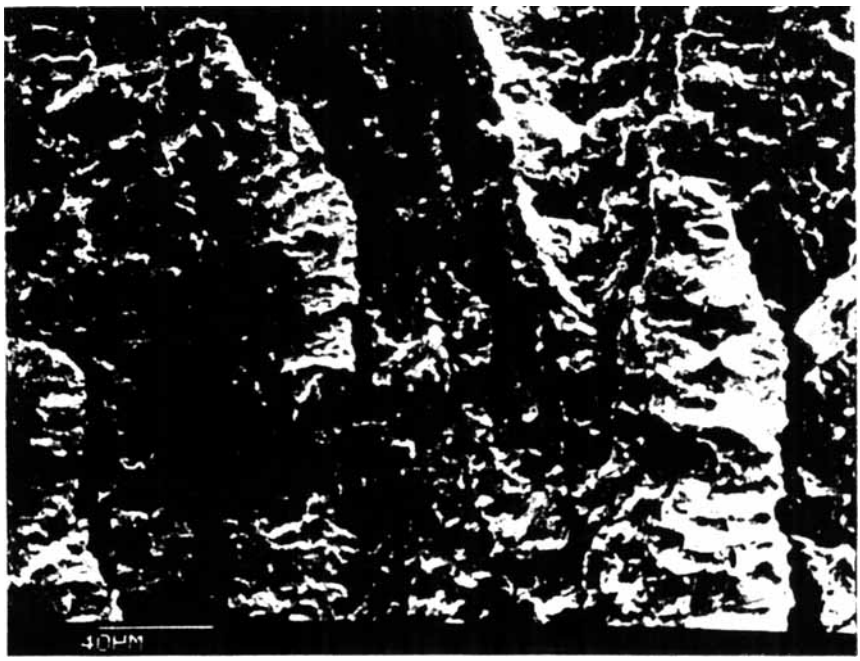

(A.2) X 400

Fig. 15. SEM photomicrographs of copolymer-type polyacetal (POM-I) at different cooling rates obtained by compression molding (A.1, A.2) at 5°C/min, (B.1, B.2) at 45°C/min, and (C.1, C.2) at 350°C/min.

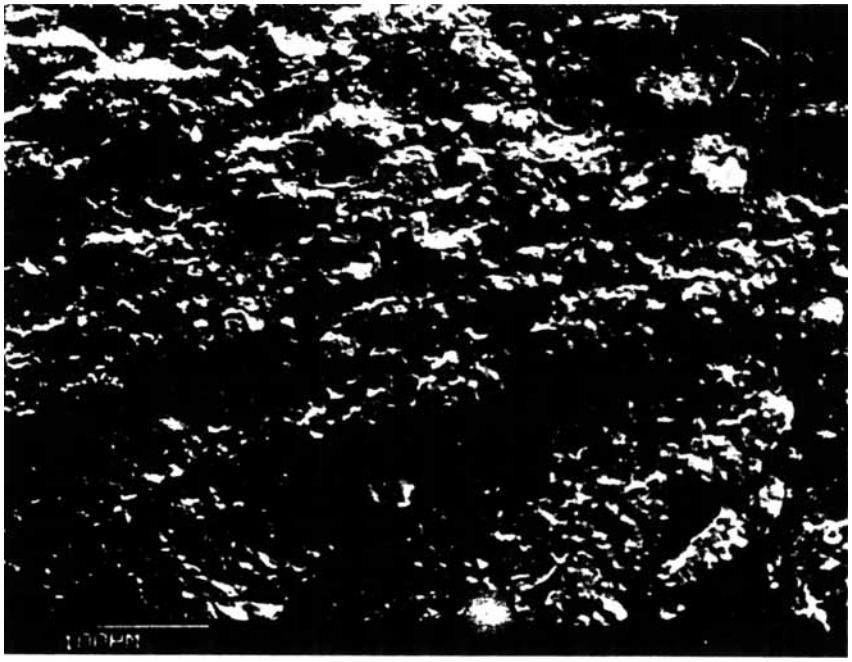

(B.1) X 150

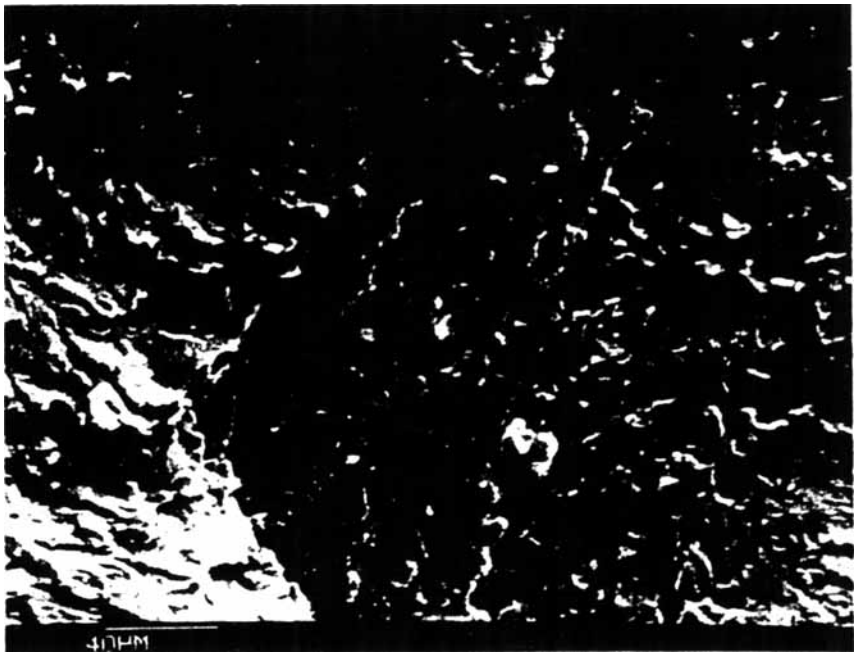

(B.2) X 400

Fig. 15. *(Continued from the previous page.)*

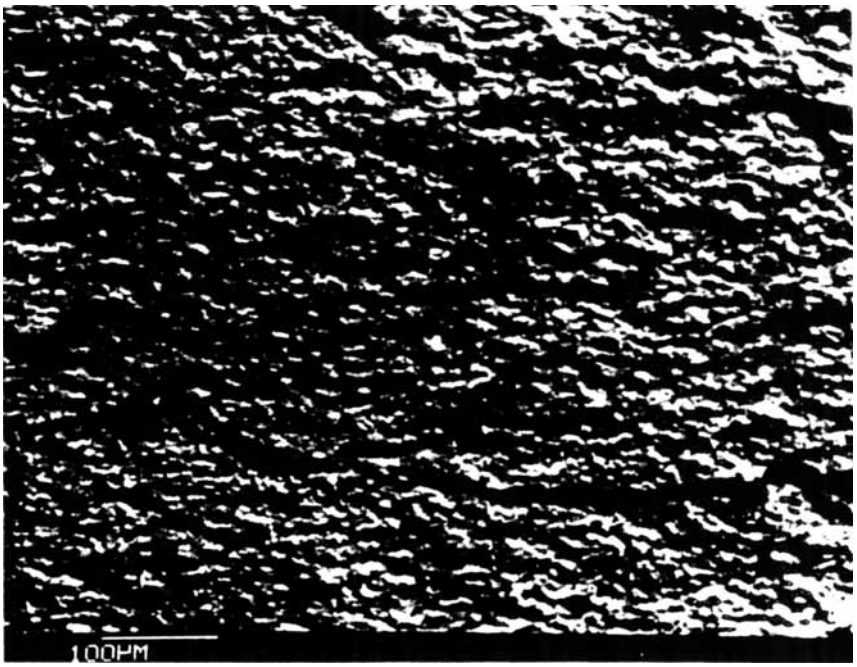

(C.1) X 150

(C.2) X 400

Fig. 15. *(Continued from the previous page.)*

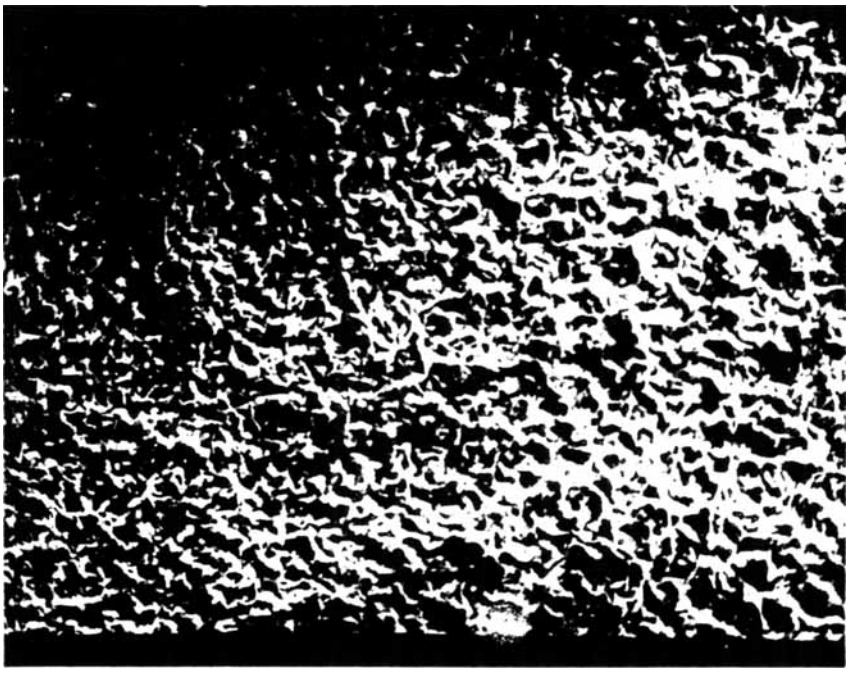

(A.1) X 150

(A.2) X 750

Fig. 16. SEM photomicrographs of acid-etched copolymer-type polyacetal (POM-I) at different cooling rates obtained by compression molding (A.1, A.2) at 5°C/min; (B.1, B.2) at 45°C/min, and (C.1, C.2) at 350°C/min.

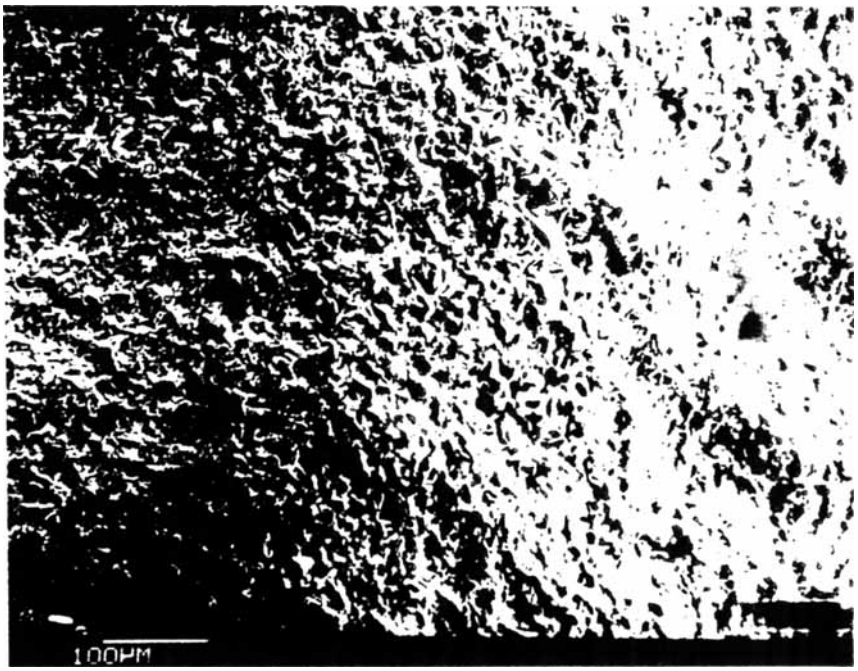

(B.1) X 150

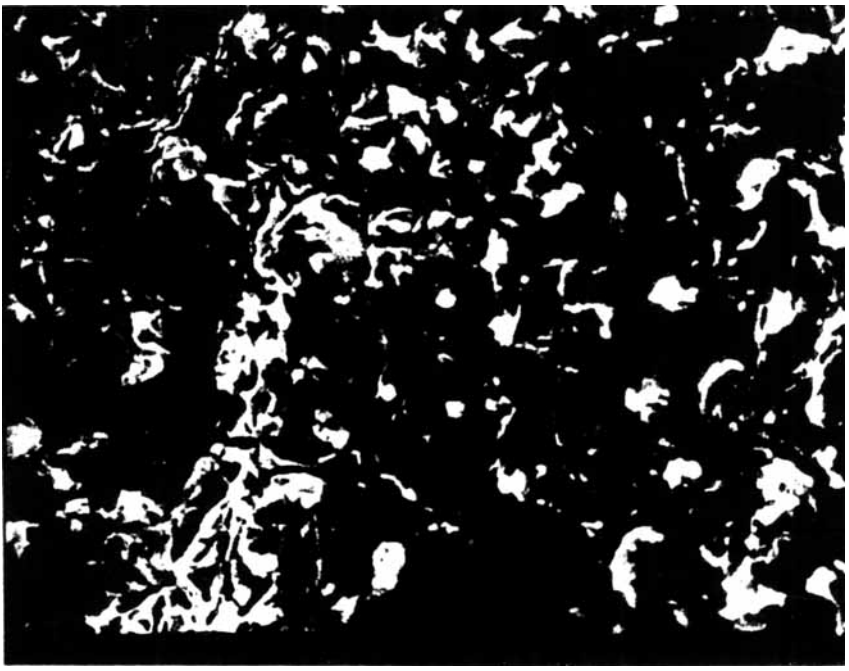

(B.2) X 750

Fig. 16. (*Continued from the previous page.*)

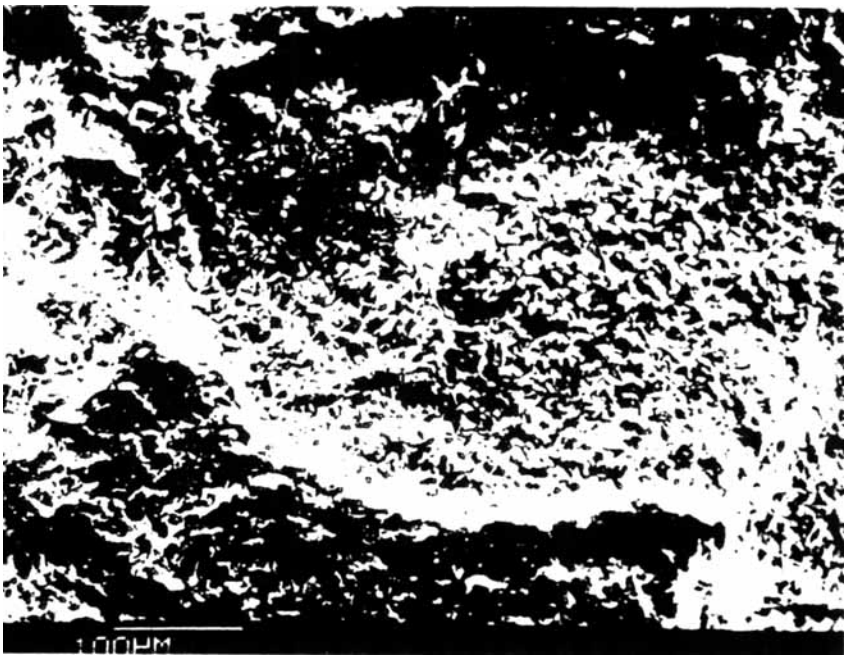

(C.1) X 150

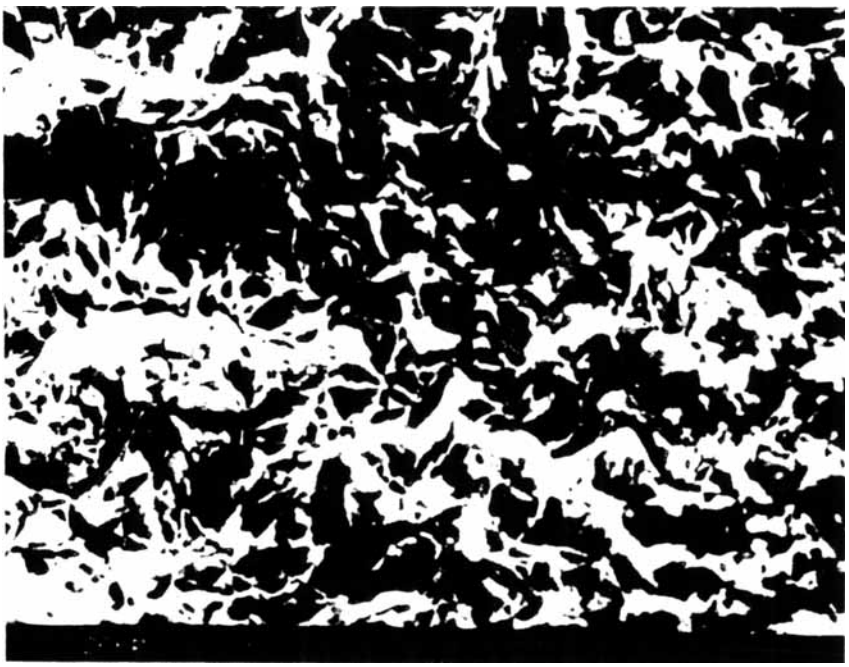

(C.2) X 750

Fig. 16. (*Continued from the previous page.*)

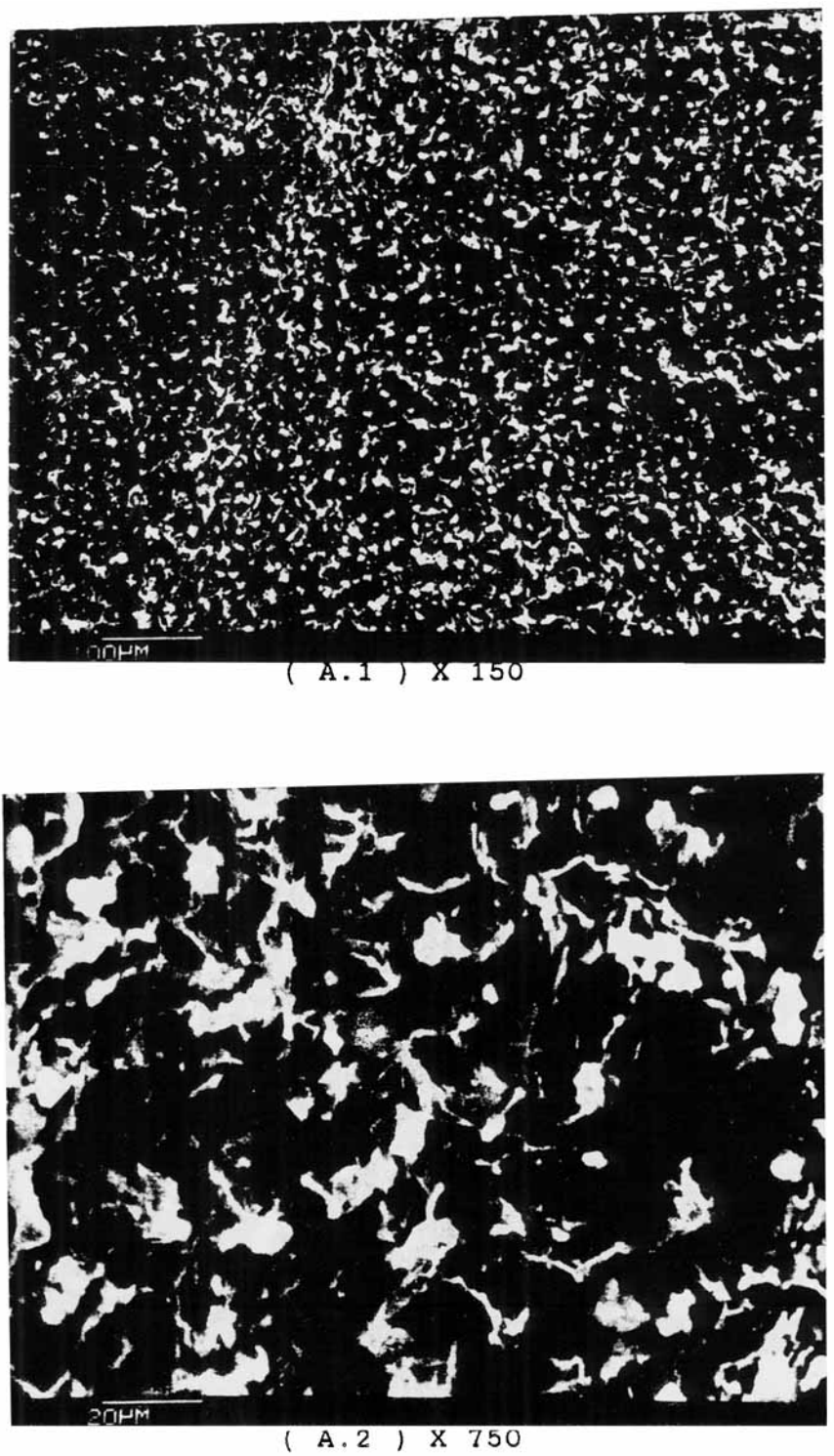

Fig. 17. SEM photomicrographs of acid-etched copolymer-type polyacetal (POM-1), annealing treatment at 150°C (A.1, A.2) for 10 min, (B.1, B.2) for 0.5 h, (C.1, C.2) for 1 h, and (D.1, D.2) for 1.5 h.

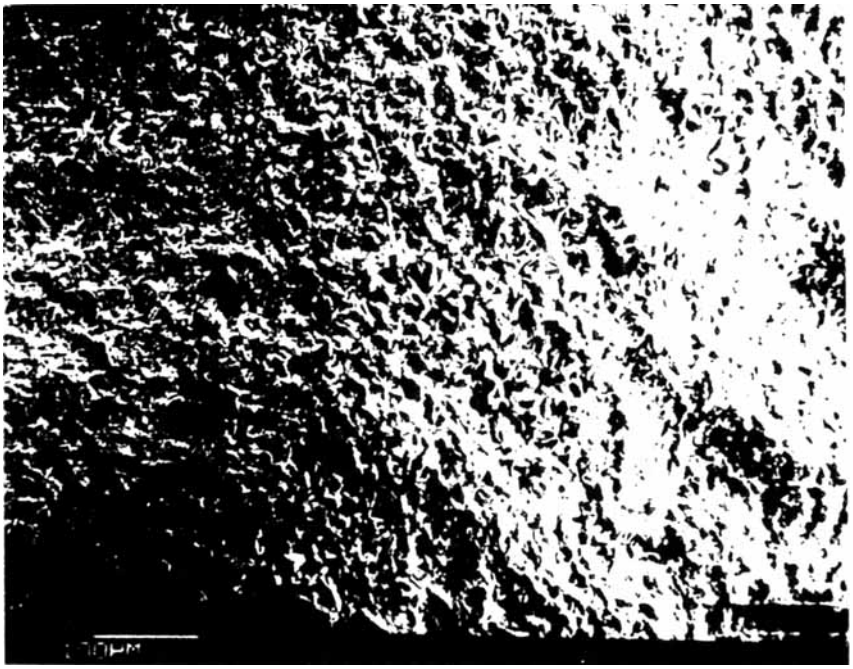

(B.1) X 150

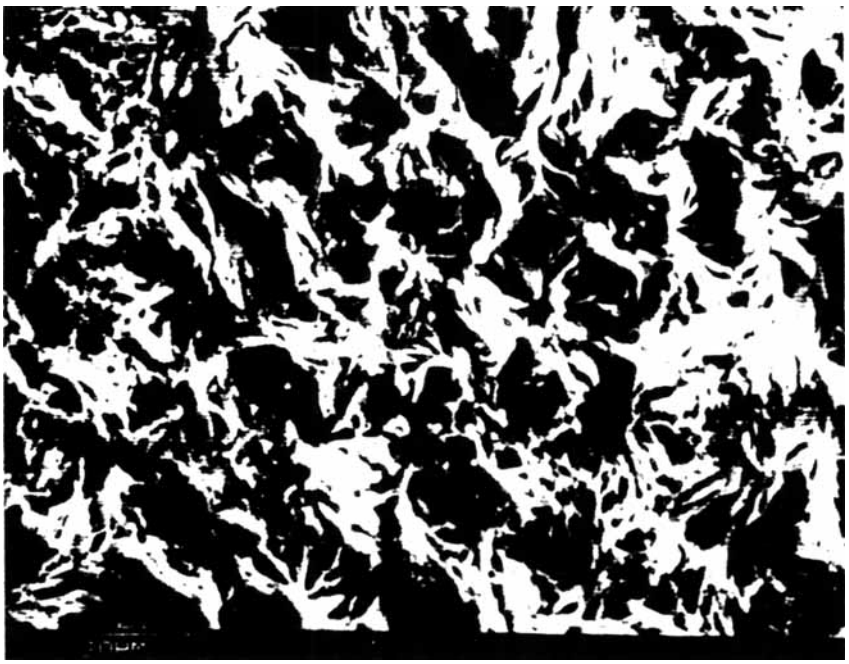

(B.2) X 750

Fig. 17. (*Continued from the previous page.*)

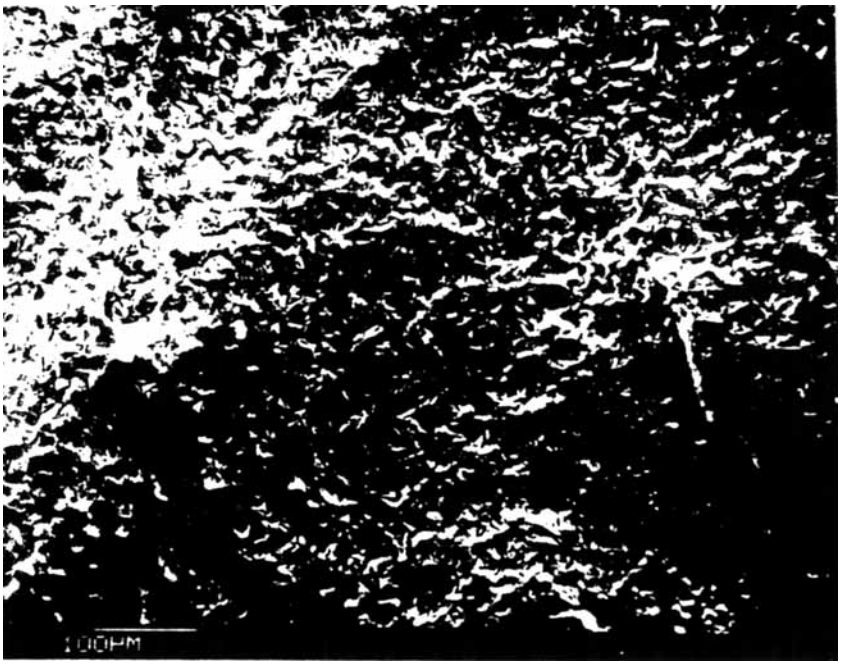

(C.1) X 150

(C.2) X 750

Fig. 17. (*Continued from the previous page.*)

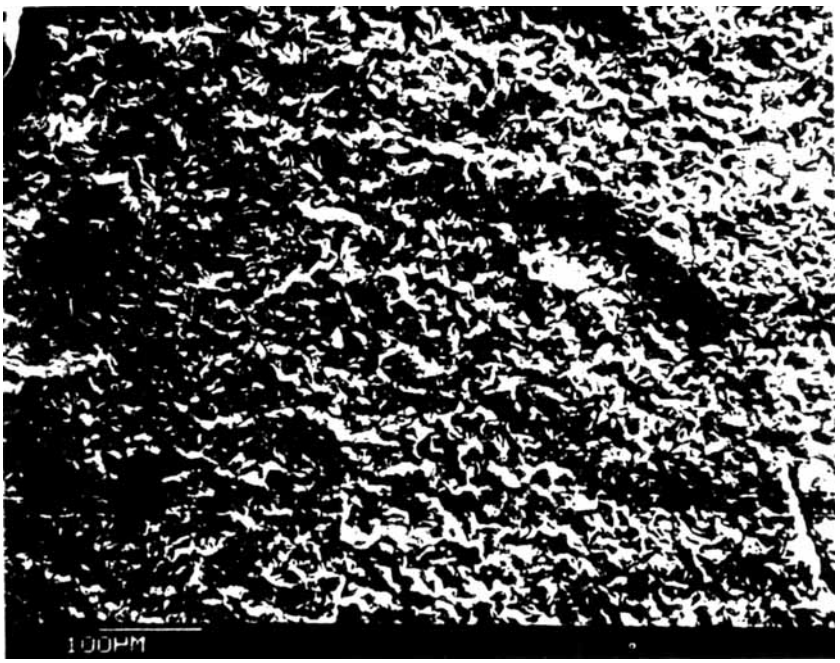

(D.1) X 150

(D.2) X 750

Fig. 17. (*Continued from the previous page.*)

easily develop larger spherulitic surface morphology. Thus the acid etchs the amorphous region faster than it does the crystalline region (Fig. 16). After the etching treatment, the POMs dimension of a smaller facetlike marking [Fig. 14(A)] is only about the diameter of one spherulite while the size of a larger facetlike marking [Fig. 14(B)] may be as large as the aggregation of two spherulite diameters. This conclusion can be applied to acid-etched fracture surface morphology of the POM (Fig. 16). Clear voids were observed on the POM surfaces which had been treated for 25 s. The appearance of the voids becomes all the more obvious if the time of etching the quickly cooled POM fracture surface by chromic acid is prolonged.[23] Clearly, a quickly cooled POM shows smaller average spherulitic surface morphology and looser packing than a slowly cooled POM.

Annealing Morphology

From the study on the crystalline structure of acid-etched fracture surface of annealed POM, it is noticed that the annealing treatment at 150°C increases the spherulitic size from 15 to 37 μm, which was calculated directly from the acid-etched fracture surface morphology in SEM (Fig. 17). Annealing a cooled POM leads to a decrease in spherulitic cavity surfaces; a result that shows apparent spherulitic surface morphology and chain extension. The effect of annealing a semicrystalline polymer with a lamellar morphology below the melting point but above the crystallization temperature shows substantial changes in molecular mobility and morphology. These changes are very likely to occur especially when the annealing time is longer, at which time the molecular mobility may be sufficiently high and the lattice sufficiently expanded, for such gliding movements.[24] It is possible to anneal the POM not only by the physical rearrangement of the macroconformation, but also by the improvement of the crystal perfection.

CONCLUSION

Heat treatment, such as slow cooling from above the melting point or annealing below the melting point but above the crystallization temperature, tends to increase the diameter of spherulitic size and crystallinity. This treatment also increases tensile strength and modulus but decreases impact strength. The effect of annealing a cooled semicrystalline polymer is believed to be a secondary recrystallization process in which there is a reorientation of parts of the crystallites. The Avrami equation enables us to evaluate the overall crystallization kinetics of copolymer-type polyacetals. The morphologies of POMs vary from disordered spherulites to well-developed spherulites. Finally, from the unetched and etched samples, larger facetlike dimensions of fracture surface may be a result of the aggregation of two spherulite diameters of the POMs. The continuing increase of the average diameter of spherulites with the prolongation of the annealing time is likely to result from a combination of several factors. The first is that recrystallization occurs at higher temperature, a fact that is well known to give thicker crystals.[22] In addition, the longer annealing time improves the crystal perfection. Therefore, the morphologies and properties of a semicrystalline polymer

are largely determined by the initial rate of cooling or a higher temperature in the course of annealing treatment.

The authors wish to express their appreciation to Dr. T. S. Lin, the President of the Tatung Institute of Technology, for his encouragement and support.

References

1. S. Hasemi and J. G. Williams, *J. Mater. Sci.*, **20**, 4202 (1985).
2. R. Connolly and R. Gauvin, *Polym. Eng. Sci.*, **25**, 548 (1985).
3. P. E. Bretz, *J. Appl. Polym. Sci.*, **27**, 1707 (1982).
4. R. W. Herhzberg, M. D. Skibo, and J. A. Manson, *J. Mater. Sci.*, **13**, 1038 (1978).
5. S. L. Kim, M. Skibo, J. A. Manson, and R. W. Hertzberg, *Polym. Eng. Sci.*, **17**, 194 (1977).
6. D. R. Fitchmun and S. Newman, *J. Polym. Sci., A-2*, **8**, 1545 (1970).
7. B. Maxwell, T. W. Hass, and W. Trice, *Polym. Eng. Sci.*, **9**, 225 (1969).
8. E. W. Fisher, *Pure Appl. Chem.*, **31**, 113 (1972).
9. D. C. Bassett and B. A. Khalifa, *Polymer*, **17**, 277 (1976).
10. K. Fujioka, *J. Appl. Polym. Sci.*, **13**, 1421 (1959).
11. S. M. Ohlberg, J. Roth, and R. A. V. Raff, *J. Appl. Polym. Sci.*, **1**, 114 (1959).
12. J. D. Hoffman and J. J. Weeks, *J. Res. Nat. Bur. Stand.*, **66A**, 13 (1963).
13. H. Wilski, *Kolloid Z*, **248**, 867 (1971).
14. D. Grenier and R. E. Prud'homme, *J. Polym. Sci., Polym. Lett. Ed.*, **18**, 1655 (1980).
15. C. J. Ong and F. P. Price, *J. Polym. Sci. Symp.*, **63**, 45 (1978).
16. F. P. Price, *J. Polym. Sci., Part A*, **3**, 3067 (1965).
17. J. N. Hay, P. A. Fitzerald, and M. Wiles, *Polymer*, **17**, 1015 (1976).
18. J. N. Hay and Z. Przekop, *J. Polym. Sci., Polym. Phy. Ed.*, **17**, 971 (1979).
19. M. C. Tobin, *J. Polym. Sci., Polym. Phys. Ed.*, **12**, 399 (1974).
20. W. O. Statton and P. H. Geil, *J. Polym. Sci.*, **3**, 357 (1960).
21. D. H. Reneker, *J. Polym. Sci.*, **59**, 539 (1962).
22. T. W. Hass, W. Trice, P. H. MacRae, and H. Pegge, *Annu. Tech. Conf., Soc. Plast. Eng., Tech. Pap.*, **15**, 16 (1969).
23. Y. Kishimoto, T. Hayashi, M. Hashimoto, and T. Ohshima, *J. Appl. Polym. Sci.*, **21**, 2740 (1977).
24. R. Hosemann, J. Loboda, H. Cackovic, and G. S. Y. Yeh, *Polymer*, **17**, 311 (1976).

Received September 16, 1986
Accepted February 23, 1987